

## Exact solution for the hypergeometric Green's function describing spectral formation in x-ray pulsars

Peter A. Becker<sup>a)</sup>

*Center for Earth Observing and Space Research, School of Computational Sciences,  
George Mason University, Fairfax, Virginia 22030-4444*

(Received 11 December 2004; accepted 17 February 2005; published online 25 April 2005)

An eigenfunction expansion method involving hypergeometric functions is used to solve the partial differential equation governing the transport of radiation in an x-ray pulsar accretion column containing a radiative shock. The procedure yields the exact solution for the Green's function, which describes the scattering of monochromatic radiation injected into the column from a source located near the surface of the star. Collisions between the injected photons and the infalling electrons cause the radiation to gain energy as it diffuses through the gas and gradually escapes by passing through the walls of the column. The presence of the shock enhances the energization of the radiation and creates a power-law spectrum at high energies, which is typical for a Fermi process. The analytical solution for the Green's function provides important physical insight into the spectral formation process in x-ray pulsars, and it also has direct relevance for the interpretation of spectral data for these sources. Additional interesting mathematical aspects of the problem include the establishment of a closed-form expression for the quadratic normalization integrals of the orthogonal eigenfunctions, and the derivation of a new summation formula involving products of hypergeometric functions. By taking various limits of the general expressions, we also develop new linear and bilinear generating functions for the Jacobi polynomials. © 2005 American Institute of Physics. [DOI: 10.1063/1.1894965]

### I. INTRODUCTION

In this paper, methods of classical analysis are employed to obtain the exact solution for the Green's function describing the spectrum of radiation emitted by an x-ray pulsar. Beyond the direct physical relevance of the Green's function, the method of solution also yields several additional results of mathematical interest, including a new summation formula involving products of two hypergeometric functions, as well as new linear and bilinear generating functions for the Jacobi polynomials. We also obtain an exact expression for the quadratic normalization integrals of the orthogonal hypergeometric eigenfunctions. Before proceeding with the main derivation, some physical background is called for. The radiation produced in bright x-ray pulsars is powered by the gravitational accretion (inflow) of ionized gas that is channeled onto the poles of a rotating neutron star by the strong magnetic field. In these sources, the radiation pressure greatly exceeds the gas pressure, and therefore the pressure of the photons governs the dynamical structure of the accretion flow. It follows that the gas must pass through a radiation-dominated shock on its way to the stellar surface, and the kinetic energy of the gas is carried away by the high-energy radiation that escapes from the column.<sup>1</sup> The strong gradient of the radiation pressure decelerates the material to rest at the surface of the star, and the compression of the infalling gas drives its temperatures up to a few million Kelvins. The gas therefore radiates x-rays, which appear to

---

<sup>a)</sup>Electronic mail: pbecker@gmu.edu

pulsate due to the star's spin. However, the observed x-ray spectrum is nonthermal, indicating that nonequilibrium processes are playing an important role in the formation of the radiation distribution.

The nonthermal shape of the spectrum is primarily due to the flow compression, which causes Fermi energization of the photons as they collide with infalling electrons in the column, until the radiation escapes from the column into space. Our primary goal in this paper is to obtain an exact solution for the Green's function describing the upscattering of soft, monoenergetic photons injected by a source located in the base of the accretion column, near the surface of the star. The Green's function contains a complete representation of the fundamental physics governing the propagation of the photons in the physical and energy spaces. Since the transport equation governing the radiation spectrum is linear, we can compute the solution associated with an arbitrary source distribution via convolution. Hence the Green's function provides the most direct means for exploring the relationship between the physics occurring in the accretion shock and the production of the observed nonthermal x radiation.

## II. FUNDAMENTAL EQUATIONS

We assume that the accretion column is cylindrical, and we define  $x$  as the spatial coordinate measured along the column axis. The gas flows through the column onto the stellar surface with velocity  $v$ . We define the Green's function,  $f_G(x_0, x, \epsilon_0, \epsilon)$ , as the radiation distribution at location  $x$  and energy  $\epsilon$  resulting from the injection of  $\dot{N}_0$  photons per second with energy  $\epsilon_0$  from a monochromatic source at location  $x_0$  inside the column. In a steady-state situation,  $f_G$  satisfies the transport equation<sup>2,3</sup>

$$v \frac{\partial f_G}{\partial x} = \frac{dv}{dx} \frac{\epsilon}{3} \frac{\partial f_G}{\partial \epsilon} + \frac{\partial}{\partial x} \left( \frac{c}{3n_e \sigma_{\parallel}} \frac{\partial f_G}{\partial x} \right) + \frac{\dot{N}_0 \delta(\epsilon - \epsilon_0) \delta(x - x_0)}{\pi r_0^2 \epsilon_0^2} - \frac{f_G}{t_{\text{esc}}} - \beta v_0 \delta(x - x_0) f_G, \quad (1)$$

where  $n_e$  is the electron number density,  $\sigma_{\parallel}$  is the electron scattering cross section for photons propagating parallel to the  $x$  axis,  $r_0$  is the radius of the column,  $v_0$  is the flow speed at the source location,  $c$  is the speed of light, and  $t_{\text{esc}}$  is the mean time photons spend in the column before escaping through the walls into space. The total radiation number and energy densities associated with the distribution function  $f_G$  are, respectively,

$$n_G(x) \equiv \int_0^{\infty} \epsilon^2 f_G d\epsilon, \quad U_G(x) \equiv \int_0^{\infty} \epsilon^3 f_G d\epsilon. \quad (2)$$

The terms in (1) represent, from left to right, the comoving (convective) time derivative, first-order Fermi energization ("bulk comptonization") of the radiation in the converging flow, spatial diffusion of the photons parallel to the column axis, the monochromatic photon source, escape of radiation from the column, and the possible absorption of radiation at the source location, respectively. In physical terms, the first-order Fermi energization corresponds to the  $P dV$  work done on the radiation by the compression of the background plasma as it accretes onto the stellar surface.<sup>3</sup> The dimensionless constant  $\beta$  expresses the strength of the absorption (if any) occurring at the source location, and the mean escape time is given by

$$t_{\text{esc}} = \frac{r_0^2 n_e \sigma_{\perp}}{c}, \quad (3)$$

where  $\sigma_{\perp}$  is the electron scattering cross section for photons propagating perpendicular to the column axis. In general,  $\sigma_{\parallel} \neq \sigma_{\perp}$  due to the influence of the strong magnetic field, which is directed parallel to the axis of the column. Absorption at the source location is expected if the photons are produced in a black-body "mound" of dense gas near the base of the accretion column,<sup>1</sup> because a perfect black body acts as both a source and a sink of radiation.<sup>4</sup>

The flux of electrons flowing down the column is denoted by  $J \equiv n_e v$ . In our cylindrical, steady-state problem,  $J$  maintains a constant value. Becker<sup>5</sup> demonstrated that in order for the inflowing matter to come to rest at the stellar surface as required, the parameters  $r_0$ ,  $J$ ,  $\sigma_{\parallel}$ , and  $\sigma_{\perp}$  must satisfy the dynamical constraint

$$r_0^2 J^2 \sigma_{\perp} \sigma_{\parallel} = \frac{3}{4} c^2. \quad (4)$$

In general, radiation-dominated shocks are continuous velocity transitions, with an overall thickness of a few Thomson scattering lengths, unlike standard (discontinuous) gas-mediated shocks.<sup>6</sup> The exact solution for the inflow velocity  $v$  as a function of the spatial coordinate  $x$  is given by<sup>5,7</sup>

$$\frac{v(x)}{v_c} = \frac{7}{4} \left[ 1 - \left( \frac{7}{3} \right)^{-1+x/x_{\text{st}}} \right], \quad (5)$$

where  $v_c$  is the flow velocity at the sonic point, which is related to the stellar mass  $M_*$ , the stellar radius  $R_*$ , and the gravitational constant  $G$  via<sup>5</sup>

$$v_c = \frac{4}{7} \left( \frac{2GM_*}{R_*} \right)^{1/2}. \quad (6)$$

The quantity  $x_{\text{st}}$  appearing in (5) is the distance between the sonic point and the stellar surface, which can be evaluated using Eq. (4.16) from Ref. 5 to obtain

$$x_{\text{st}} = \frac{r_0}{2\sqrt{3}} \left( \frac{\sigma_{\perp}}{\sigma_{\parallel}} \right)^{1/2} \ln \left( \frac{7}{3} \right). \quad (7)$$

According to (5), the flow does come to rest at the surface of the star as required, since  $v(x_{\text{st}}) = 0$ . Furthermore, the constancy of the electron flux  $J$  in our cylindrical, steady-state problem implies that the electron number density  $n_e$  is a function of  $x$  because  $v$  varies with the height inside the column [see Eq. (5)].

Further simplification is possible if we work in terms of the new spatial variable  $y$ , defined by

$$y(x) \equiv \left( \frac{7}{3} \right)^{-1+x/x_{\text{st}}}. \quad (8)$$

Note that  $y \rightarrow 0$  in the far upstream region ( $x \rightarrow -\infty$ ), and  $y \rightarrow 1$  at the surface of the star ( $x \rightarrow x_{\text{st}}$ ). Based on (5) and (8), we find that the variation of the velocity  $v$  as a function of the new variable  $y$  is given by the simple expression

$$\frac{v(y)}{v_c} = \frac{7}{4} (1 - y). \quad (9)$$

By combining (3), (4), and (9) with the derivative relation

$$\frac{dx}{dy} = \frac{r_0}{2\sqrt{3}} \left( \frac{\sigma_{\perp}}{\sigma_{\parallel}} \right)^{1/2} y^{-1}, \quad (10)$$

we can transform the transport equation (1) for  $f_G$  from  $x$  to  $y$  to obtain

$$y(1-y) \frac{\partial^2 f_G}{\partial y^2} + \left( \frac{1-5y}{4} \right) \frac{\partial f_G}{\partial y} - \frac{\epsilon}{4} \frac{\partial f_G}{\partial \epsilon} + \left( \frac{y-1}{4y} \right) f_G = \frac{3\beta v_0 \delta(y-y_0) f_G}{7v_c} - \frac{3\dot{N}_0 \delta(\epsilon - \epsilon_0) \delta(y-y_0)}{7\pi r_0^2 \epsilon_0^2 v_c}, \quad (11)$$

where  $y_0 \equiv y(x_0)$  denotes the value of  $y$  at the source location. According to (9), the flow velocity at the source,  $v_0$ , is related to  $v_c$  and  $y_0$  by

$$\frac{v_0}{v_c} = \frac{7}{4}(1 - y_0). \quad (12)$$

Note that we can write the Green's function as either  $f_G(x_0, x, \epsilon_0, \epsilon)$  or  $f_G(y_0, y, \epsilon_0, \epsilon)$  since the parameters  $(x, x_0)$  and  $(y, y_0)$  are interchangeable via (8).

### III. SOLUTION FOR THE GREEN'S FUNCTION

The physical model considered here includes Fermi energization, which tends to boost the energy of the injected photons as they collide with high-energy electrons streaming down through the accretion column towards the surface of the neutron star. Moreover, since no process that can lower the photon energy is included in the model, all of the photons injected from a source of monochromatic radiation with energy  $\epsilon = \epsilon_0$  must at later times have energy  $\epsilon > \epsilon_0$ . It follows that  $f_G = 0$  for  $\epsilon < \epsilon_0$ . When  $\epsilon > \epsilon_0$ , (11) is separable in energy and space using the functions

$$f_\lambda(\epsilon, y) = \epsilon^{-\lambda} g(\lambda, y), \quad (13)$$

where  $\lambda$  is the separation constant, and the spatial function  $g$  satisfies the differential equation

$$y(1-y) \frac{d^2 g}{dy^2} + \left( \frac{1-5y}{4} \right) \frac{dg}{dy} + \left( \frac{\lambda y + y - 1}{4y} \right) g = \frac{3\beta v_0 \delta(y - y_0)}{7v_c} g. \quad (14)$$

In order to avoid an infinite spatial diffusion flux at  $y = y_0$ , the function  $g$  must be continuous there, and consequently we obtain the condition

$$\Delta[g(\lambda, y)]|_{y=y_0} \equiv \lim_{\epsilon \rightarrow 0} g(\lambda, y_0 + \epsilon) - g(\lambda, y_0 - \epsilon) = 0. \quad (15)$$

We can also derive a jump condition for the derivative  $dg/dy$  at the source location by integrating (14) with respect to  $y$  in a small region around  $y = y_0$ . The result obtained is

$$\Delta \left[ \frac{dg}{dy} \right] \Big|_{y=y_0} = \frac{3\beta}{4y_0} g(\lambda, y_0), \quad (16)$$

where we have used (12) to substitute for  $v_0$ .

The homogeneous version of (14) obtained when  $y \neq y_0$  has fundamental solutions given by

$$\varphi_1(\lambda, y) \equiv yF(a, b; c; y), \quad (17)$$

$$\varphi_1^*(\lambda, y) \equiv y^{-1/4} F(a - 5/4, b - 5/4; 2 - c; y), \quad (18)$$

where  $F(a, b; c; z)$  denotes the hypergeometric function,<sup>8</sup> and the parameters  $a$ ,  $b$ , and  $c$  are defined by

$$a \equiv \frac{9 - \sqrt{17 + 16\lambda}}{8}, \quad b \equiv \frac{9 + \sqrt{17 + 16\lambda}}{8}, \quad c \equiv \frac{9}{4}, \quad (19)$$

and therefore  $a + b = c$ .

#### A. Asymptotic analysis

The source photons injected into the flow are unable to diffuse very far upstream due to the high speed of the inflowing electrons. Most of the photons escape through the walls of the column within a few scattering lengths of the source, and therefore we conclude that the function  $g$  must *vanish* in the upstream limit,  $y \rightarrow 0$ . Asymptotic analysis indicates that the function  $\varphi_1(\lambda, y) \rightarrow 0$  in the limit  $y \rightarrow 0$  as required, but  $\varphi_1^*(\lambda, y)$  diverges and therefore it cannot be utilized in the upstream region ( $y \leq y_0$ ). Hence  $g$  must be given by  $\varphi_1$  for  $y \leq y_0$ . Conversely, in the downstream limit, the gas settles onto the surface of the star and therefore  $g$  should approach a constant as  $y \rightarrow 1$ . These

conditions are satisfied if  $\lambda$  is equal to one of the eigenvalues,  $\lambda_n$ , which are associated with the spatial eigenfunctions,  $g_n(y)$ , defined by

$$g_n(y) \equiv g(\lambda_n, y). \quad (20)$$

In order to obtain a complete understanding of the global behavior of the eigenfunctions, we must also consider the asymptotic behaviors of the two functions  $\varphi_1$  and  $\varphi_1^*$  in the downstream region, which are discussed below.

The hypergeometric functions appearing in (17) and (18) can be evaluated at  $y=1$  using Eq. (15.1.20) from Abramowitz and Stegun,<sup>8</sup> which gives for general values of  $a$ ,  $b$ , and  $c$ ,

$$F(a, b; c; 1) = \frac{\Gamma(c)\Gamma(c-a-b)}{\Gamma(c-a)\Gamma(c-b)}. \quad (21)$$

However, for the values of  $a$ ,  $b$ , and  $c$  in (17) and (18), we find that [see Eq. (19)]

$$c - a - b = 0, \quad (22)$$

and therefore the hypergeometric functions  $F(a, b; c; y)$  and  $F(a-5/4, b-5/4; 2-c; y)$  each *diverge* in the downstream limit  $y \rightarrow 1$ . Since the eigenfunction  $g_n$  should approach a constant as  $y \rightarrow 1$  based on physical considerations, we conclude that in the downstream region ( $y \geq y_0$ ),  $g_n$  must be represented by a suitable linear combination of  $\varphi_1$  and  $\varphi_1^*$  that remains *finite* as  $y \rightarrow 1$ . In order to make further progress, we need to employ Eq. (15.3.10) from Abramowitz and Stegun,<sup>8</sup> which yields for general  $a$ ,  $b$ , and  $y$ ,

$$F(a, b; a+b; y) = \frac{\Gamma(a+b)}{\Gamma(a)\Gamma(b)} \sum_{n=0}^{\infty} \frac{(a)_n (b)_n}{(n!)^2} [2\Psi(n+1) - \Psi(a+n) - \Psi(b+n) - \ln(1-y)] (1-y)^n, \quad (23)$$

where

$$\Psi(z) \equiv \frac{1}{\Gamma(z)} \frac{d\Gamma(z)}{dz}. \quad (24)$$

Asymptotic analysis of this expression reveals that in the limit  $y \rightarrow 1$ , the logarithmic divergences of the two functions  $\varphi_1$  and  $\varphi_1^*$  can be balanced by creating the new function

$$\varphi_2(\lambda, y) \equiv \frac{\Gamma(b)}{\Gamma(c)\Gamma(1-b)} \varphi_1(\lambda, y) - \frac{\Gamma(1-a)}{\Gamma(2-c)\Gamma(a)} \varphi_1^*(\lambda, y), \quad (25)$$

which remains finite as  $y \rightarrow 1$ . Hence  $\varphi_2$  represents the fundamental solution for  $g_n$  in the region downstream from the source. We can use the asymptotic behaviors of  $\varphi_1$  and  $\varphi_1^*$  to show that

$$\lim_{y \rightarrow 1} \varphi_2(\lambda, y) = \frac{\pi[\cot(\pi a) + \cot(\pi b)]}{\Gamma(a)\Gamma(1-b)}. \quad (26)$$

Since the solutions  $\varphi_1$  and  $\varphi_2$  are applicable in the upstream and downstream regions, respectively, the global expression for the eigenfunction  $g_n$  is therefore given by

$$g_n(y) = \begin{cases} \varphi_1(\lambda_n, y), & y \leq y_0, \\ B_n \varphi_2(\lambda_n, y), & y \geq y_0, \end{cases} \quad (27)$$

where the constant  $B_n$  is evaluated using the continuity condition [Eq. (15)], which yields

$$B_n = \frac{\varphi_1(\lambda_n, y_0)}{\varphi_2(\lambda_n, y_0)}. \quad (28)$$

It follows from (26)–(28) that the downstream value of  $g_n$  is given by

$$\lim_{y \rightarrow 1} g_n(y) = \frac{\pi[\cot(\pi a) + \cot(\pi b)]}{\Gamma(a)\Gamma(1-b)} \frac{\varphi_1(\lambda_n, y_0)}{\varphi_2(\lambda_n, y_0)}. \quad (29)$$

Conversely, in the upstream region,  $\varphi_1 \rightarrow y$ , and therefore we have the asymptotic behavior

$$\lim_{y \rightarrow 0} \frac{g_n(y)}{y} = 1. \quad (30)$$

## B. Eigenvalue equation

We can combine (16), (27), and (28) to show that the eigenvalues  $\lambda_n$  satisfy the equation

$$W(\lambda_n, y_0) - \frac{3\beta\varphi_1(\lambda_n, y_0)\varphi_2(\lambda_n, y_0)}{4y_0} = 0, \quad (31)$$

where the Wronskian of the two functions  $\varphi_1$  and  $\varphi_2$  is defined for general values of  $\lambda$  and  $y$  by

$$W(\lambda, y) \equiv \varphi_1 \frac{d\varphi_2}{dy} - \varphi_2 \frac{d\varphi_1}{dy}. \quad (32)$$

Further progress can be made by deriving an analytical expression for the Wronskian. We begin by writing the differential equation (14) governing the two functions  $\varphi_1$  and  $\varphi_2$  in the self-adjoint form

$$\frac{d}{dy} \left[ y^{1/4}(1-y) \frac{d\varphi}{dy} \right] + \frac{\lambda}{4y^{3/4}} \varphi - T\varphi = 0, \quad (33)$$

where

$$T \equiv \frac{1-y}{4y^{7/4}} + \frac{3\beta v_0 \delta(y-y_0)}{7v_c y^{3/4}}. \quad (34)$$

By applying (33) to the function  $\varphi_2$  and multiplying the result by  $\varphi_1$ , and then subtracting from this the same expression with  $\varphi_1$  and  $\varphi_2$  interchanged, we obtain

$$\varphi_1 \frac{d}{dy} \left[ y^{1/4}(1-y) \frac{d\varphi_2}{dy} \right] - \varphi_2 \frac{d}{dy} \left[ y^{1/4}(1-y) \frac{d\varphi_1}{dy} \right] = 0, \quad (35)$$

which can be rewritten as

$$y^{1/4}(1-y) \frac{dW}{dy} + W \frac{d}{dy} [y^{1/4}(1-y)] = 0, \quad (36)$$

where we have made use of the result

$$\frac{dW}{dy} = \varphi_1 \frac{d^2\varphi_2}{dy^2} - \varphi_2 \frac{d^2\varphi_1}{dy^2}. \quad (37)$$

Equation (36) can be rearranged in the form

$$\frac{d \ln W}{dy} = -\frac{d}{dy} \ln[y^{1/4}(1-y)], \quad (38)$$

which can be integrated to obtain the exact solution

$$W(\lambda, y) = \frac{D(\lambda)}{y^{1/4}(1-y)}, \quad (39)$$

where  $D(\lambda)$  is an integration constant that depends on  $\lambda$  but not on  $y$ . The exact dependence of  $D$  on  $\lambda$  can be derived by analyzing the behaviors of the functions  $\varphi_1$  and  $\varphi_2$  in the limit  $y \rightarrow 0$ . For small values of  $y$ , we have the asymptotic expressions<sup>8</sup>

$$\varphi_1 \rightarrow y, \quad y \rightarrow 0,$$

$$\varphi_2 \rightarrow -\frac{\Gamma(1-a)}{\Gamma(a)\Gamma(2-c)}y^{-1/4}, \quad y \rightarrow 0. \quad (40)$$

Combining (32) and (40), we find that asymptotically,

$$W \rightarrow \frac{5}{4} \frac{\Gamma(1-a)}{\Gamma(a)\Gamma(2-c)}y^{-1/4}, \quad y \rightarrow 0. \quad (41)$$

Comparing this result with (39), we conclude that

$$D(\lambda) = \frac{5}{4} \frac{\Gamma(1-a)}{\Gamma(a)\Gamma(2-c)}, \quad (42)$$

and therefore the exact solution for the Wronskian for general values of  $\lambda$  and  $y$  is given by

$$W(\lambda, y) = \frac{5}{4} \frac{\Gamma(1-a)}{\Gamma(a)\Gamma(2-c)} \frac{y^{-1/4}}{1-y}. \quad (43)$$

Substituting for  $W$  in (31) using (43), we can rewrite the eigenvalue equation in the equivalent form

$$\frac{5}{3} \frac{\Gamma(1-a)}{\Gamma(a)\Gamma(2-c)} \frac{y_0^{3/4}}{1-y_0} = \beta \varphi_1(\lambda_n, y_0) \varphi_2(\lambda_n, y_0), \quad (44)$$

where  $a$  and  $b$  are functions of  $\lambda_n$  by virtue of (19), and  $c=9/4$ . The roots of this expression are the eigenvalues  $\lambda_n$ , and the associated eigenfunctions are evaluated using (27). The first eigenvalue,  $\lambda_0$ , is especially important because it determines the power-law shape of the high-energy portion of the Green's function [see Eq. (13)].

In Fig. 1 we plot the first eigenvalue  $\lambda_0$  as a function of the dimensionless parameters  $\beta$  and  $y_0$ . Note that  $\lambda_0$  is a double-valued function of  $y_0$  for fixed  $\beta$ , which is a consequence of the imposed velocity profile [Eq. (5)]. Physically, this behavior reflects the fact that it is always possible to achieve a desired amount of compression (first-order Fermi energization) by placing the source in a specific location in either the upstream or downstream regions of the flow. We also observe that if we increase the absorption parameter  $\beta$  while holding  $y_0$  fixed, then  $\lambda_0$  increases monotonically, and therefore the high-energy spectrum becomes progressively steeper. This behavior is expected physically because as the absorption parameter is increased, the injected photons spend less time on average being energized by collisions with electrons before either escaping from the column or being absorbed at the source location. The decreased amount of energization naturally leads to a steepening of the radiation spectrum. When  $\beta=0$ , no absorption occurs, and the index  $\lambda_0$  achieves its minimum (limiting) value of 4. This limit is, however, unphysical since

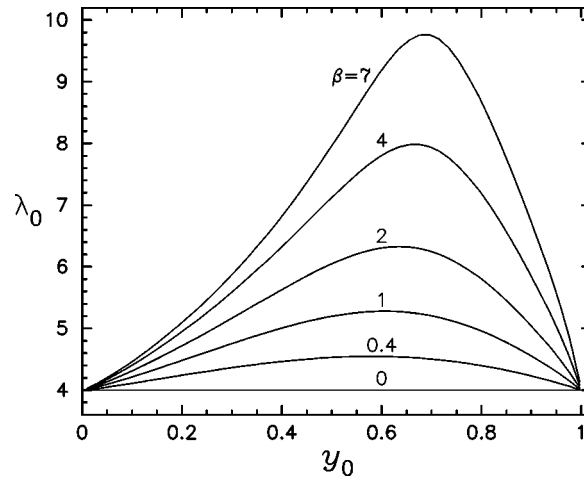


FIG. 1. First eigenvalue  $\lambda_0$  of the Green's function expansion plotted as a function of the source location  $y_0$  for the indicated values of the absorption parameter  $\beta$ . Note the steepening of the radiation spectrum that occurs when  $\beta$  is increased for a fixed value of  $y_0$ , which reflects the decreasing residence time for the photons in the plasma (see the discussion in the text).

it yields a divergent result for the total photon energy density  $U_G$  according to (2). Nonetheless, the case with  $\beta=0$  is interesting from a mathematical viewpoint, and for that reason it is further discussed in Sec. V.

### C. Orthogonality of the eigenfunctions

We shall next demonstrate that the eigenfunctions  $g_n(y)$  form an orthogonal set, which is an extremely useful property. This is a standard Sturm–Liouville problem and therefore we follow the usual procedure. Let us suppose that  $g_n(y)$  and  $g_m(y)$  are two eigenfunctions corresponding to the distinct eigenvalues  $\lambda_n$  and  $\lambda_m$ , respectively. The functions  $g_n$  and  $g_m$  each satisfy the differential equation (14), and therefore we can utilize the self-adjoint form to write [cf. Eq. (33)]

$$g_m \left\{ \frac{d}{dy} \left[ y^{1/4}(1-y) \frac{dg_n}{dy} \right] + \frac{\lambda_n}{4y^{3/4}} g_n - T g_n \right\} = 0 \quad (45)$$

and

$$g_n \left\{ \frac{d}{dy} \left[ y^{1/4}(1-y) \frac{dg_m}{dy} \right] + \frac{\lambda_m}{4y^{3/4}} g_m - T g_m \right\} = 0, \quad (46)$$

where  $T$  is given by (34). Subtracting the second equation from the first yields, after integrating by parts with respect to  $y$  from  $y=0$  to  $y=1$ ,

$$(\lambda_n - \lambda_m) \int_0^1 y^{-3/4} g_n(y) g_m(y) dy = 4y^{1/4}(1-y) \left[ g_n \frac{dg_m}{dy} - g_m \frac{dg_n}{dy} \right] \Big|_0^1. \quad (47)$$

Based on the asymptotic behaviors of the eigenfunctions  $g_n$  and  $g_m$  given by (29) and (30), we find that the right-hand side of (47) vanishes exactly, and therefore we obtain

$$(\lambda_n - \lambda_m) \int_0^1 y^{-3/4} g_n(y) g_m(y) dy = 0, \quad (48)$$

which establishes the orthogonality of the eigenfunctions. The set of eigenfunctions is also complete according to the Sturm–Liouville theorem. Since the eigenfunctions are orthogonal, the Green's function can be expressed as the infinite series

$$f_G(y_0, y, \epsilon_0, \epsilon) = \sum_{n=0}^{\infty} A_n \left( \frac{\epsilon}{\epsilon_0} \right)^{-\lambda_n} g_n(y), \quad (49)$$

for  $\epsilon \geq \epsilon_0$ , where the expansion coefficients  $A_n$  are computed by employing the orthogonality of the eigenfunctions along with the condition

$$f_G(y_0, y, \epsilon_0, \epsilon)|_{\epsilon=\epsilon_0} = \frac{12\dot{N}_0}{7\pi r_0^2 \epsilon_0^3 v_c} \delta(y - y_0), \quad (50)$$

which is obtained by integrating the transport equation (11) with respect to  $\epsilon$  in a small range surrounding the injection energy  $\epsilon_0$ . The result obtained for the  $n$ th expansion coefficient is

$$A_n = \frac{12\dot{N}_0 y_0^{-3/4} g_n(y_0)}{7\pi r_0^2 \epsilon_0^3 v_c \mathfrak{C}_n}, \quad (51)$$

where the quadratic normalization integrals,  $\mathfrak{C}_n$ , are defined by

$$\mathfrak{C}_n \equiv \int_0^1 y^{-3/4} g_n^2(y) dy. \quad (52)$$

As an alternative to numerical integration, in Sec. III D we derive a closed-form expression for evaluating the normalization integrals based directly on the associated differential equation.

#### D. Quadratic normalization integrals

The direct computation of the normalization integrals  $\mathfrak{C}_n$  via numerical integration is costly and time consuming, and therefore it is desirable to have an alternative procedure available for their evaluation. In fact, it is possible to derive an analytical expression for the normalization integrals based on manipulation of the fundamental differential equation (14) governing the eigenfunctions  $g_n(y)$ .

Let us suppose that  $g(\lambda, y)$  is a general solution to (14) for an arbitrary value of  $\lambda$  (i.e., not necessarily an eigenvalue) with the asymptotic (upstream) behavior

$$g(\lambda, y) \rightarrow y, \quad y \rightarrow 0, \quad (53)$$

which is the same as the upstream behavior of the eigenfunction  $g_n(y)$  [see Eq. (30)]. We also stipulate that  $g$  must be continuous at  $y=y_0$ , and that it satisfies the derivative jump condition given by (16). After a bit of algebra, we find that the global solution for  $g$  consistent with these requirements can be expressed as

$$g(\lambda, y) = \begin{cases} \varphi_1(\lambda, y), & y \leq y_0, \\ (1 + \hat{a})\varphi_1(\lambda, y) + \hat{b}\varphi_2(\lambda, y), & y \geq y_0, \end{cases} \quad (54)$$

where the coefficients  $\hat{a}$  and  $\hat{b}$  are given by

$$\hat{a} = -\frac{3\beta\varphi_1(\lambda, y_0)\varphi_2(\lambda, y_0)}{4y_0W(\lambda, y_0)}, \quad \hat{b} = \frac{3\beta\varphi_1^2(\lambda, y_0)}{4y_0W(\lambda, y_0)}, \quad (55)$$

and the Wronskian  $W$  is evaluated using (43).

Comparing the general solution for  $g(\lambda, y)$  with the solution for the eigenfunction  $g_n(y)$  given by (27), we note that

$$\lim_{\lambda \rightarrow \lambda_n} \hat{a} = -1, \quad \lim_{\lambda \rightarrow \lambda_n} \hat{b} = B_n. \quad (56)$$

We can now use the self-adjoint form of (14) to write [cf. Eqs. (45) and (46)]

$$g_n \left\{ \frac{\partial}{\partial y} \left[ y^{1/4}(1-y) \frac{\partial g}{\partial y} \right] + \frac{\lambda}{4y^{3/4}} g - Tg \right\} = 0 \quad (57)$$

and

$$g \left\{ \frac{d}{dy} \left[ y^{1/4}(1-y) \frac{dg_n}{dy} \right] + \frac{\lambda_n}{4y^{3/4}} g_n - Tg_n \right\} = 0, \quad (58)$$

where  $T$  is defined by (34). Subtracting the second equation from the first and integrating by parts from  $y=0$  to  $y=1$  yields

$$(\lambda - \lambda_n) \int_0^1 y^{-3/4} g(\lambda, y) g_n(y) dy = 4y^{1/4}(1-y) \left[ g(\lambda, y) \frac{dg_n}{dy} - g_n(y) \frac{\partial g}{\partial y} \right] \Big|_0^1. \quad (59)$$

Since  $g \rightarrow y$  and  $g_n \rightarrow y$  as  $y \rightarrow 0$ , we conclude that the evaluation at the lower bound  $y=0$  on the right-hand side yields zero, and consequently in the limit  $\lambda \rightarrow \lambda_n$  we obtain for the quadratic normalization integral  $\mathfrak{C}_n$  [see Eq. (52)],

$$\mathfrak{C}_n = \int_0^1 y^{-3/4} g_n^2(y) dy = \lim_{\lambda \rightarrow \lambda_n} \frac{4y^{1/4}(1-y) [g(\lambda, y) (dg_n/dy) - g_n(y) (\partial g/\partial y)]}{\lambda - \lambda_n} \Big|_{y=1}. \quad (60)$$

The numerator and denominator on the right-hand side of (60) each vanish in the limit  $\lambda \rightarrow \lambda_n$ , and therefore we can employ L'Hôpital's rule to show that (e.g., Becker<sup>9</sup>)

$$\mathfrak{C}_n = \lim_{\lambda \rightarrow \lambda_n} 4y^{1/4}(1-y) \left[ \frac{\partial g}{\partial y} \frac{dg_n}{dy} - g_n \frac{\partial^2 g}{\partial y \partial \lambda} \right] \Big|_{y=1}. \quad (61)$$

Substituting the analytical forms for  $g_n(y)$  and  $g(\lambda, y)$  given by (27) and (54), respectively, we find that (61) can be rewritten as

$$\mathfrak{C}_n = \lim_{y \rightarrow 1} 4y^{1/4}(1-y) B_n \left[ W(\lambda, y) \frac{d\hat{a}}{d\lambda} + B_n \frac{\partial \varphi_2}{\partial \lambda} \frac{\partial \varphi_2}{\partial y} - B_n \varphi_2(\lambda, y) \frac{\partial^2 \varphi_2}{\partial y \partial \lambda} \right] \Big|_{\lambda=\lambda_n}, \quad (62)$$

where we have also utilized (32) and (56). Based on the asymptotic behavior of  $\varphi_2$  [see (26)], we conclude that the final two terms on the right-hand side of (62) contribute nothing in the limit  $y \rightarrow 1$ , and therefore our expression for  $\mathfrak{C}_n$  reduces to

$$\mathfrak{C}_n = \lim_{y \rightarrow 1} 4y^{1/4}(1-y) B_n W(\lambda, y) \frac{d\hat{a}}{d\lambda} \Big|_{\lambda=\lambda_n}. \quad (63)$$

Since  $y=1$  is a singular point of the differential equation (14), it is convenient to employ the relation [see Eq. (39)]

$$W(\lambda, y) y^{1/4}(1-y) = W(\lambda, y_0) y_0^{1/4}(1-y_0), \quad (64)$$

which allows us to transform the evaluation in (63) from  $y=1$  to  $y=y_0$  to obtain the equivalent result

$$\mathfrak{C}_n = 4y_0^{1/4}(1-y_0) \hat{a} W(\lambda, y_0) \frac{\varphi_1(\lambda_n, y_0)}{\varphi_2(\lambda_n, y_0)} \frac{d \ln \hat{a}}{d\lambda} \Big|_{\lambda=\lambda_n}, \quad (65)$$

where we have also substituted for  $B_n$  using (28). The derivative on the right-hand side can be evaluated using (55), which yields

$$\frac{d \ln \hat{a}}{d\lambda} = \frac{\partial \ln \varphi_1}{\partial \lambda} + \frac{\partial \ln \varphi_2}{\partial \lambda} - \frac{\partial \ln W}{\partial \lambda}, \quad (66)$$

where the derivative of the Wronskian is given by [see Eqs. (19) and (43)]

$$\frac{\partial \ln W}{\partial \lambda} = \frac{\Psi(a) + \Psi(1-a)}{(17+16\lambda)^{1/2}} \quad (67)$$

and

$$\Psi(z) \equiv \frac{1}{\Gamma(z)} \frac{d\Gamma(z)}{dz}. \quad (68)$$

Combining (55) and (65)–(67), we find that the quadratic normalization integrals can be evaluated using the closed-form expression

$$\mathfrak{C}_n = K(\lambda_n, y_0), \quad (69)$$

where

$$K(\lambda, y) \equiv 3\beta y^{-3/4}(1-y)\varphi_1^2(\lambda, y) \left[ \frac{\Psi(a) + \Psi(1-a)}{(17+16\lambda)^{1/2}} - \frac{\partial \ln \varphi_1}{\partial \lambda} - \frac{\partial \ln \varphi_2}{\partial \lambda} \right]. \quad (70)$$

This formula provides an extremely efficient alternative to numerical integration for the computation of  $\mathfrak{C}_n$ .

## E. Numerical examples

In this section we illustrate the computational method by examining the dependence of the Green's function  $f_G(y_0, y, \epsilon_0, \epsilon)$  on the spatial location  $y$  and the energy  $\epsilon$ . We remind the reader that the solution for the Green's function represents the photon spectrum inside the accretion column at the specified position and energy, resulting from the injection of monochromatic photons with energy  $\epsilon_0$  from a source located at  $y_0$ . Hence analysis of  $f_G$  allows us to explore the competing effects of Fermi energization and diffusion as photons travel through the column. The Green's function can be computed by combining (49), (51), and (69) once the eigenvalues  $\lambda_n$  have been determined using (44). The eigenfunction expansion for  $f_G$  converges fairly rapidly, and in general one obtains at least five decimal digits of accuracy if the series in (49) is terminated after the first 20 terms.

The Green's function  $f_G(y_0, y, \epsilon_0, \epsilon)$  is plotted as a function of the energy ratio  $\epsilon/\epsilon_0$  and the location  $y$  in Fig. 2 for the parameter values  $\beta=0.4$  and  $y_0=0.9$ . In this case the first eigenvalue is given by  $\lambda_0=4.231$  (see Fig. 1), which is equal to the high-energy slope of the Green's function in the log–log plots in Fig. 2. The selected value of  $y_0$  corresponds to a source located near the bottom of the accretion column, just above the stellar surface. At the source location,  $y=y_0=0.9$ , the energy spectrum extends down to the injection energy,  $\epsilon_0$ . However, at all other radii the spectrum displays a steep turnover above that energy because all of the photons have experienced Fermi energization due to collisions with the infalling electrons. The photons with energy  $\epsilon=\epsilon_0$  at the source location have been injected so recently that they have not yet experienced significant energization. Note that in the far upstream region (i.e., for small values of  $y$ ), the spectrum is greatly attenuated due to the inability of the photons to diffuse upstream through the rapidly infalling plasma. In this example, the average photon energy achieves its maximum value in the upstream region because these are the photons that have resided in the flow the longest and therefore experienced the most energy amplification. However, due to the attenuation mentioned above, there are not many of these photons.

In Fig. 3 we plot the Green's function  $f_G$  for the case with  $\beta=4$  and  $y_0=0.4$ , which yields for the first eigenvalue  $\lambda_0=6.325$ . The source is now located in the upstream region and the absorption is stronger, and consequently the behavior is somewhat different from that displayed in Fig. 2. In

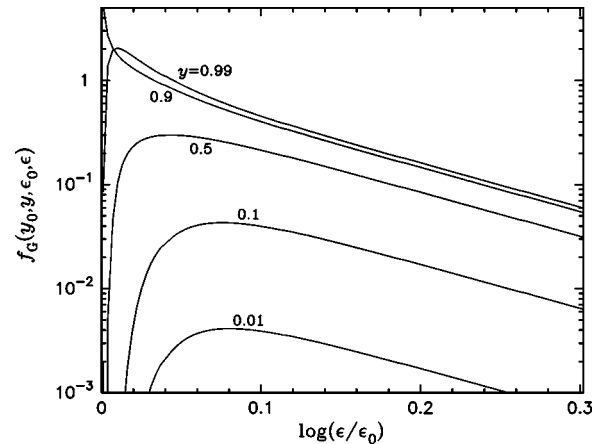


FIG. 2. Green's function  $f_G(y_0, y, \epsilon_0, \epsilon)$  [Eq. (49)] plotted in units of  $\dot{N}_0/(v_0^2 \epsilon_0^3 v_c)$  as a function of the photon energy ratio  $\epsilon/\epsilon_0$  for the indicated values of the spatial variable  $y$ . In this example we have set the absorption constant  $\beta=0.4$  and the source location parameter  $y_0=0.9$ , so that the source is located near the base of the accretion column.

particular, the photons experience less overall compression in the flow and therefore the spectrum is steeper at high energies, as evidenced by the increase in the primary eigenvalue  $\lambda_0$ . This is mainly due to the larger value of  $\beta$ , which causes the photons to spend less time on average in the flow being energized by collisions with the electrons before they escape from the column or are “recycled” by absorption. We also note that in this case the average radiation energy displays its maximum value in the downstream region. This is the reverse of the behavior displayed in Fig. 2 because in the present situation, the source is located in the upstream region and therefore the photons that diffuse further upstream do not experience as much energization as those considered in Fig. 2. The radiation distribution in the far upstream region is greatly attenuated due to diffusion against the current of infalling electrons, as in Fig. 2. The analytical results for the Green's function obtained here provide the basis for the consideration of any source distribution since the fundamental differential equation (1) is linear. This is further discussed in Sec. IV.

#### IV. HYPERGEOMETRIC SUMMATION FORMULA

We can derive two interesting summation formulas for the hypergeometric eigenfunctions by using the transport equation (11) to study the behavior of the “energy moments,”  $I_\ell$ , defined by

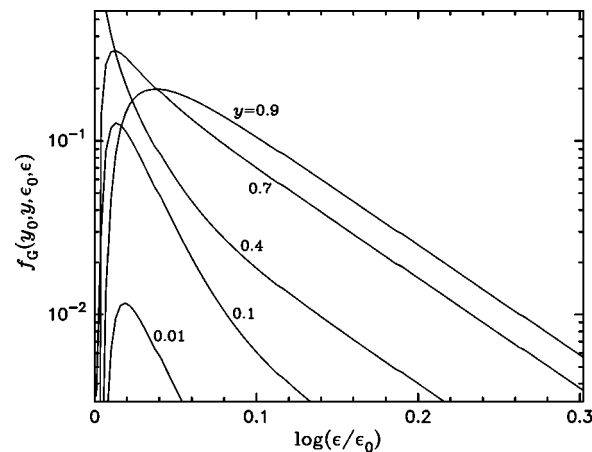


FIG. 3. Same as Fig. 2, except  $\beta=4.0$  and  $y_0=0.4$ . In this case the source is located in the upstream region, and the average photon energy achieves its maximum value in the downstream region.

$$I_\ell(y) \equiv \int_{\epsilon_0}^{\infty} \epsilon^\ell f_G d\epsilon. \quad (71)$$

The lower bound of  $\epsilon_0$  is chosen because  $f_G=0$  for  $\epsilon < \epsilon_0$  as explained in the discussion preceding (13). Note that according to (2), the number and energy densities are given by  $n_G=I_2$  and  $U_G=I_3$ , respectively. The differential equation satisfied by  $I_\ell$  is obtained by operating on (11) with  $\int \epsilon^\ell d\epsilon$ , which yields

$$y(1-y) \frac{d^2 I_\ell}{dy^2} + \left( \frac{1-5y}{4} \right) \frac{dI_\ell}{dy} + \left( \frac{\ell y + 2y - 1}{4y} \right) I_\ell = \frac{3\beta v_0 \delta(y-y_0) I_\ell}{7v_c} - \frac{3\dot{N}_0 \epsilon_0^{\ell-2} \delta(y-y_0)}{7\pi r_0^2 v_c}. \quad (72)$$

The energy moment  $I_\ell$  must be continuous at  $y=y_0$  in order to avoid generating an infinite spatial diffusion flux there, and consequently we have

$$\Delta [I_\ell(y)]|_{y=y_0} = 0. \quad (73)$$

By integrating (72) in a small region around  $y=y_0$ , we can show that  $I_\ell$  also satisfies the derivative jump condition

$$\Delta \left[ \frac{dI_\ell}{dy} \right] \Big|_{y=y_0} = \frac{3\beta I_\ell(y_0)}{4y_0} - \frac{3\dot{N}_0 \epsilon_0^{\ell-2}}{7\pi r_0^2 v_c y_0 (1-y_0)}, \quad (74)$$

where we have also utilized (12).

The homogeneous version of (72) obtained when  $y \neq y_0$  is equivalent to (14) for  $g$  if we replace  $\lambda$  with  $\ell+1$ . Since the energy moments  $I_\ell$  must satisfy the same upstream and downstream boundary conditions that apply to the separation eigenfunctions  $g_n$ , we can therefore write the general solution for  $I_\ell$  as

$$I_\ell(y) = \begin{cases} C_\ell \varphi_1(\ell+1, y), & y \leq y_0, \\ D_\ell \varphi_2(\ell+1, y), & y \geq y_0, \end{cases} \quad (75)$$

where the constants  $C_\ell$  and  $D_\ell$  are computed by satisfying the continuity and derivative jump conditions given by (73) and (74). Upon substitution, we obtain after some algebra

$$C_\ell = \frac{12\dot{N}_0 \epsilon_0^{\ell-2}}{7\pi v_c r_0^2} \frac{(1-y_0)^{-1} \varphi_2(\ell+1, y_0)}{3\beta \varphi_1(\ell+1, y_0) \varphi_2(\ell+1, y_0) - 4y_0 W(\ell+1, y_0)}, \quad (76)$$

$$D_\ell = \frac{12\dot{N}_0 \epsilon_0^{\ell-2}}{7\pi v_c r_0^2} \frac{(1-y_0)^{-1} \varphi_1(\ell+1, y_0)}{3\beta \varphi_1(\ell+1, y_0) \varphi_2(\ell+1, y_0) - 4y_0 W(\ell+1, y_0)}, \quad (77)$$

where  $W(\ell+1, y_0)$  is computed using [cf. Eq. (43)]

$$W(\ell+1, y_0) = \frac{5}{4} \frac{\Gamma(1-a_\ell)}{\Gamma(a_\ell)\Gamma(-1/4)} \frac{y_0^{-1/4}}{1-y_0} \quad (78)$$

and

$$a_\ell \equiv \frac{9 - \sqrt{33 + 16\ell}}{8}. \quad (79)$$

The energy moments  $I_\ell(y)$  can also be calculated by substituting for the Green's function in the fundamental integral (71) using (49). Reversing the order of summation and integration yields

$$I_\ell(y) = \epsilon_0^{\ell+1} \sum_{n=0}^{\infty} A_n (\lambda_n - \ell - 1)^{-1} g_n(y), \quad (80)$$

where  $g_n(y)$  and  $A_n$  are given by (27) and (51), respectively. Note that the expression for  $g_n(y)$  can be rewritten as

$$g_n(y) = \frac{\varphi_1(\lambda_n, y_{\min}) \varphi_2(\lambda_n, y_{\max})}{\varphi_2(\lambda_n, y_0)}, \quad (81)$$

where

$$y_{\min} \equiv \min(y, y_0), \quad y_{\max} \equiv \max(y, y_0). \quad (82)$$

Eliminating  $I_\ell(y)$  between (75) and (80) and making use of (51), (76), (77), and (81), we find after some simplification that

$$\sum_{n=0}^{\infty} \frac{\varphi_1(\lambda_n, y_0)}{\varphi_2(\lambda_n, y_0)} \frac{\varphi_1(\lambda_n, y_{\min}) \varphi_2(\lambda_n, y_{\max})}{(\lambda_n - \ell - 1) \mathfrak{E}_n} = \frac{y_0^{3/4} (1 - y_0)^{-1} \varphi_1(\ell + 1, y_{\min}) \varphi_2(\ell + 1, y_{\max})}{3\beta \varphi_1(\ell + 1, y_0) \varphi_2(\ell + 1, y_0) - 4y_0 W(\ell + 1, y_0)}, \quad (83)$$

where the eigenvalues  $\lambda_n$  are computed using (44). Equation (83) is a new hypergeometric summation formula that has not appeared previously in the literature. This relation holds for all real values of  $\ell$ .

## V. LINEAR AND BILINEAR GENERATING FUNCTIONS

The case with  $\beta=0$  is interesting from a mathematical point of view because in this limit, the hypergeometric eigenfunctions reduce to Jacobi polynomials. We can therefore combine various results from Secs. III and IV to obtain two new summation formulas (i.e., linear and bilinear generating functions) for the Jacobi polynomials that have not appeared previously in the literature. In the limit  $\beta \rightarrow 0$ , the eigenvalue equation (31) reduces to

$$W(\lambda_n, y_0) = \frac{5}{4} \frac{\Gamma(1-a)}{\Gamma(a)\Gamma(-1/4)} \frac{y_0^{-1/4}}{1-y_0} = 0, \quad (84)$$

where we have also made use of (43). Roots of this expression occur where  $|\Gamma(a)| \rightarrow \infty$ , which corresponds to

$$a = -n, \quad n = 0, 1, 2, \dots \quad (85)$$

In this situation, we can use (19) to demonstrate that the exact solution for the eigenvalues  $\lambda_n$  is given by

$$\lambda_n = 4n^2 + 9n + 4. \quad (86)$$

Next we note that  $a+b=9/4$  in general according to (19), and therefore we find that

$$b = \frac{9}{4} + n. \quad (87)$$

The corresponding expression for the fundamental upstream eigensolution,  $\varphi_1(\lambda_n, y)$ , is given in this case by the polynomial [see Eq. (17)]

$$\varphi_1(\lambda_n, y) = yF\left(-n, \frac{9}{4} + n; \frac{9}{4}; y\right), \quad (88)$$

and the fundamental eigensolution in the downstream region,  $\varphi_2(\lambda_n, y)$ , likewise reduces to [see Eq. (25)]

$$\varphi_2(\lambda_n, y) = \frac{\Gamma(n+9/4)}{\Gamma(9/4)\Gamma(-n-5/4)} \varphi_1(\lambda_n, y). \quad (89)$$

Hence the two eigensolutions  $\varphi_1(\lambda_n, y)$  and  $\varphi_2(\lambda_n, y)$  are *linearly dependent functions* in this case, which is expected since the Wronskian  $W(\lambda_n, y_0) = 0$  according to (84). This in turn reflects the fact that there is no derivative jump in the global separation eigenfunction  $g_n(y)$  at  $y = y_0$  when  $\beta = 0$  [see Eq. (16)].

Due to the linear dependence of  $\varphi_1(\lambda_n, y)$  and  $\varphi_2(\lambda_n, y)$ , Eq. (81) for the global eigenfunction  $g_n(y)$  now simplifies to

$$g_n(y) = \varphi_1(\lambda_n, y), \quad (90)$$

and therefore the summation formula presented in (83) can be rewritten in the  $\beta = 0$  case as

$$\sum_{n=0}^{\infty} \frac{\varphi_1(\lambda_n, y_0) \varphi_1(\lambda_n, y)}{(\lambda_n - \ell - 1) \mathfrak{C}_n} = - \frac{\varphi_1(\ell + 1, y_{\min}) \varphi_2(\ell + 1, y_{\max})}{4y_0^{1/4} (1 - y_0) W(\ell + 1, y_0)}, \quad (91)$$

where  $y_{\min}$  and  $y_{\max}$  are defined by (82) and  $W(\ell + 1, y_0)$  is computed using (78).

We are now in a position to derive an interesting summation formula for products of Jacobi polynomials. Using Eq. (15.4.6) from Abramowitz and Stegun,<sup>8</sup> our expression for the eigensolution  $\varphi_1(\lambda_n, y)$  can be rewritten as

$$\varphi_1(\lambda_n, y) = \frac{n!}{(9/4)_n} y P_n^{(5/4, 0)}(1 - 2y), \quad (92)$$

where

$$P_n^{(5/4, 0)}(1 - 2y) = \frac{(9/4)_n}{n!} F\left(-n, \frac{9}{4} + n; \frac{9}{4}; y\right) \quad (93)$$

represents the Jacobi polynomial, and  $(a)_n$  denotes the Pochhammer symbol, defined by<sup>8</sup>

$$(a)_n \equiv \frac{\Gamma(a+n)}{\Gamma(a)}. \quad (94)$$

In the present application, with  $\beta = 0$ , we can combine (52), (90), and (92) to express the quadratic normalization integrals,  $\mathfrak{C}_n$ , as

$$\mathfrak{C}_n = \left[ \frac{n!}{(9/4)_n} \right]^2 \int_0^1 y^{5/4} [P_n^{(5/4, 0)}(1 - 2y)]^2 dy, \quad (95)$$

which can be evaluated using Eq. (7.391.1) from Gradshteyn and Ryzhik<sup>10</sup> to obtain

$$\mathfrak{C}_n = \left[ \frac{n!}{(9/4)_n} \right]^2 \left( 2n + \frac{9}{4} \right)^{-1}. \quad (96)$$

Equations (78), (86), (91), (92), and (96) can be combined to derive a new *bilinear generating function* for the Jacobi polynomials, which can be written as

$$\sum_{n=0}^{\infty} (9 + 8n) \frac{P_n^{(5/4, 0)}(1 - 2y_0) P_n^{(5/4, 0)}(1 - 2y)}{4n^2 + 9n + 3 - \ell} = \frac{16 \Gamma(3/4) \Gamma(a_\ell)}{5 \Gamma(1 - a_\ell)} \frac{\varphi_1(\ell + 1, y_{\min}) \varphi_2(\ell + 1, y_{\max})}{y y_0}, \quad (97)$$

where  $a_\ell$  is defined by (79). Note that the functions  $\varphi_1(\ell + 1, y_{\min})$  and  $\varphi_2(\ell + 1, y_{\max})$  appearing on the right-hand side of (97) are *not* eigenfunctions since in general the quantity  $\ell + 1$  is not equal to one of the eigenvalues  $\lambda_n$ .

An interesting special case occurs in the limit  $y_0 \rightarrow 0$ . Making use of the relation [see Eq. (93)]

$$P_n^{(5/4,0)}(1) = \frac{(9/4)_n}{n!}, \quad (98)$$

and the identity

$$\Gamma\left(\frac{3}{4}\right)\Gamma\left(\frac{9}{4}\right) = \frac{5}{16}\pi 2^{1/2}, \quad (99)$$

we now find that (97) reduces to the *linear generating function*

$$\sum_{n=0}^{\infty} \frac{(9+8n)\Gamma(n+9/4)}{(4n^2+9n+3-\ell)n!} P_n^{(5/4,0)}(1-2y) = \frac{\pi 2^{1/2}\Gamma(a_\ell)}{\Gamma(1-a_\ell)} \frac{\varphi_2(\ell+1, y)}{y}, \quad (100)$$

which is valid for all real values of  $\ell$ . Equations (97) and (100) are new results that are useful for the evaluation of infinite sums containing either products of Jacobi polynomials or single Jacobi polynomials, respectively.

## VI. CONCLUSION

In this paper we have employed methods of classical analysis to obtain the exact solution for the Green's function describing the Fermi energization of photons scattered by infalling electrons in a pulsar accretion column. This process is of central importance in the development of theoretical models for the production of the x-ray spectra observed from these objects, which are among the brightest sources in the Milky Way galaxy. As demonstrated in Fig. 1 and Eq. (49), the Green's function is characterized by a power-law shape at high photon energies, which is typical for a Fermi process. In this scenario, photons gain their energy by diffusing back and forth across the shock many times. The probability of multiple shock crossings decreases exponentially with the number of crossings, and the mean energy of the photons increases exponentially with the number of crossings. This combination of factors naturally gives rise to a power-law energy distribution.<sup>11</sup> Hence shock energization in the pulsar accretion column provides a simple explanation for the spectrum of the high-energy radiation produced by x-ray pulsars. Specific examples of the Green's function are plotted in Figs. 2 and 3.

Due to the linearity of the transport equation (1), we can employ the Green's function to calculate the radiation spectrum inside the accretion column resulting from an arbitrary source spectrum using the convolution<sup>12</sup>

$$f(y_0, y, \epsilon) = \int_0^\infty j(\epsilon_0) \frac{f_G(y_0, y, \epsilon_0, \epsilon)}{\dot{N}_0} d\epsilon_0, \quad (101)$$

where  $j(\epsilon_0)d\epsilon_0$  represents the number of photons injected per unit time into the accretion column at location  $y_0$  with energy between  $\epsilon_0$  and  $\epsilon_0+d\epsilon_0$ . The source distribution of greatest astrophysical interest is the "thermal mound" source located near the base of the accretion column, where the gas has decelerated almost to rest and is therefore extremely dense. This hot plasma is in full thermodynamic equilibrium, and consequently it radiates a black-body spectrum.<sup>1</sup> The absorption parameter  $\beta$  has been included in the transport equation (1) in order to account for the fact that a black body acts as both a source and a sink of radiation.<sup>4</sup> The fundamental results for the Green's function obtained in the present paper will be used to study the reprocessing of the black-body radiation emitted from the thermal mound in a subsequent paper.

In addition to the analytical results for the Green's function, we have also obtained an interesting formula for the evaluation of an infinite series involving products of the orthogonal hypergeometric eigenfunctions [see Eq. (83)]. This derivation was based on the simultaneous calculation of the energy moments  $I_\ell(y)$  using both an expression based on term-by-term integration of the Green's function expansion (49), and an independent solution developed via direct integration of the fundamental transport equation (1). In the special case  $\beta \rightarrow 0$ , which corresponds physically

to the neglect of absorption at the source location, our general formula for the hypergeometric summation reduces to a bilinear generating function for the Jacobi polynomials given by (97). This relation in turn simplifies to yield a linear generating function for the Jacobi polynomials in the limit  $y_0 \rightarrow 0$ , which corresponds physically to a source located in the far upstream region [see Eq. (100)].

The results derived in this paper for the linear and bilinear generating functions of Jacobi polynomials are related to various similar expressions obtained previously by Chen and Srivastava,<sup>13,14</sup> Srivastava,<sup>15</sup> Rangarajan,<sup>16</sup> and Pittaluga, Sacripante, and Srivastava.<sup>17</sup> However, our results are not identical to any of their formulas and therefore they represent an interesting new family of relations. Although the linear and bilinear generating functions developed here relate specifically to the properties of the polynomials  $P_n^{(5/4,0)}(1-2y)$ , we expect that some level of generalization may be possible. We plan to pursue this question in future work.

<sup>1</sup>K. Davidson, *Nature (London), Phys. Sci.* **246**, 1 (1973).

<sup>2</sup>P. A. Becker, *Astrophys. J.* **397**, 88 (1992).

<sup>3</sup>P. A. Becker and M. T. Wolff, *Astrophys. J. Lett.* **621**, L45 (2005).

<sup>4</sup>G. B. Rybicki and A. P. Lightman, *Radiative Processes in Astrophysics* (Wiley, New York, 1979).

<sup>5</sup>P. A. Becker, *Astrophys. J.* **498**, 790 (1998).

<sup>6</sup>R. D. Blandford and D. G. Payne, *Mon. Not. R. Astron. Soc.* **194**, 1041 (1981).

<sup>7</sup>M. M. Basko and R. A. Sunyaev, *Mon. Not. R. Astron. Soc.* **175**, 395 (1976).

<sup>8</sup>M. Abramowitz and I. A. Stegun, *Handbook of Mathematical Functions* (Dover, New York, 1970).

<sup>9</sup>P. A. Becker, *J. Math. Phys.* **38**, 3692 (1997).

<sup>10</sup>I. S. Gradshteyn and I. M. Ryzhik, *Table of Integrals, Series, and Products* (Academic, London, 1980).

<sup>11</sup>E. Fermi, *Astrophys. J.* **119**, 1 (1954).

<sup>12</sup>P. A. Becker, *Mon. Not. R. Astron. Soc.* **343**, 215 (2003).

<sup>13</sup>M.-P. Chen and H. M. Srivastava, *J. Appl. Math. Stoch. Anal.* **8**, 423 (1995).

<sup>14</sup>M.-P. Chen and H. M. Srivastava, *Appl. Math. Comput.* **68**, 153 (1995).

<sup>15</sup>H. M. Srivastava, *Proc. Natl. Acad. Sci. U.S.A.* **64**, 462 (1969).

<sup>16</sup>S. K. Rangarajan, *Bull. Acad. Pol. Sci., Ser. Sci., Math., Astron. Phys.* **13**, 101 (1965).

<sup>17</sup>G. Pittaluga, L. Sacripante, and H. M. Srivastava, *J. Math. Anal. Appl.* **238**, 385 (1999).